

# Blind Diagnosis for Millimeter-wave Massive MIMO Systems

Rui Sun, Weidong Wang, Li Chen, Guo Wei, and Wenyi Zhang, *Senior Member, IEEE*

**Abstract**—Millimeter-wave (mmWave) massive multiple-input-multiple-output (MIMO) systems rely on large-scale antenna arrays to combat large path-loss at mmWave band. Due to hardware characteristics and deploying environments, mmWave massive MIMO systems are vulnerable to antenna element blockages and failures, which necessitate diagnostic techniques to locate faulty antenna elements for calibration purposes. Current diagnostic techniques require full or partial knowledge of channel state information (CSI), which can be challenging to acquire in the presence of antenna failures. In this letter, we propose a blind diagnostic technique to identify faulty antenna elements in mmWave massive MIMO systems, which does not require any CSI knowledge. By jointly exploiting the sparsity of mmWave channel and failure, we first formulate the diagnosis problem as a joint sparse recovery problem. Then, the atomic norm is introduced to induce the sparsity of mmWave channel over continuous Fourier dictionary. An efficient algorithm based on alternating direction method of multipliers (ADMM) is proposed to solve the proposed problem. Finally, the performance of proposed technique is evaluated through numerical simulations.

**Index Terms**—Array diagnosis, atomic norm, fault identification, massive MIMO, millimeter-wave communication

## I. INTRODUCTION

Millimeter-wave (mmWave) massive multiple-input-multiple-output (MIMO) system is a key technology in current and next-generation mobile communication systems, which may suffer from antenna element failures due to hardware characteristics and deploying environments. MmWave active devices like amplifiers and mixers are generally less reliable than conventional sub-6G devices due to higher operating frequency and lower power efficiency [1], [2]. Besides, mmWave antenna elements are susceptible to blockages with comparable sizes like dirt and precipitation owing to the short wavelength at the mmWave band [3]. The existence of antenna element failure will cause signal power reduction and radiation pattern distortion, which may lead to severe degradation in system performance. Therefore, diagnostic techniques for mmWave massive MIMO systems are of great significance for system monitoring and maintenance.

Extensive related works on the antenna array diagnosis have been proposed, including compressed sensing based ones [4]–[10] and deep learning based one [11]. The main idea of compressed sensing based diagnostic techniques is to use known channel state information (CSI) to generate fault-free reference signal and then subtract it from the received signal.

Therefore, the differential signal contains the information of faulty antenna elements, which can be estimated from compressed measurements. The work [4] was the first to introduce compressed sensing to the array diagnosis. Improvements over [4] include modifications in sampling methods [5]–[7] and refinements in sparse recovery algorithms [8]–[10]. In particular, the work in [12] extended the above antenna-only diagnosis to the joint diagnosis of antenna, phase shifter, and RF chain for hybrid beamforming (HBF) systems. Deep-learning based diagnostic techniques include [11], which utilizes a convolutional neural network (CNN) to detect the abnormality in the distribution of received signal and then locate faulty antenna elements.

In order to distinguish antenna failure from channel fading, the above diagnostic techniques rely on perfect CSI to generate fault-free reference signal, which can be challenging to acquire in the presence of antenna failures. Recently, a diagnostic technique proposed in [13] relaxes the CSI requirement, which only needs the angle-of-arrival (AOA) of each sub-path in the channel, i.e., partial CSI. However, acquiring the AOA of each sub-path still can be a challenging task for a potentially faulty system since faulty antenna elements will change array geometry and distort radiation pattern, which makes AOA estimation highly unreliable.

Aiming at this limitation, in this letter, we propose a blind diagnostic technique for mmWave massive MIMO systems. The term ‘blind’ represents that the proposed technique does not require any knowledge of the CSI, which is achieved by jointly exploiting the sparsity of the mmWave channel and the failure. Specifically, we first formulate the diagnosis problem as a joint sparse recovery problem. Then, the atomic norm is introduced to induce the sparsity of mmWave channel over the continuous Fourier dictionary. An efficient algorithm based on alternating direction method of multipliers (ADMM) is proposed to solve the joint sparse recovery problem. Finally, numerical simulations validate the proposed technique. To the best of our knowledge, this work is the first to propose a diagnostic technique that does not require any knowledge of the CSI.

**Notations:** We use a lowercase and an uppercase bold letter to represent a vector and a matrix, respectively.  $\|\mathbf{a}\|_1$  and  $\|\mathbf{a}\|_2$  represent the  $l_1$  and  $l_2$  norm of the vector  $\mathbf{a}$ , respectively. In particular,  $\|\mathbf{a}\|_{\mathcal{A}}$  denotes the atomic norm of  $\mathbf{a}$ . For a matrix  $\mathbf{A}$ ,  $\mathbf{A}^T$ ,  $\mathbf{A}^H$  denote the transpose and conjugate transpose of  $\mathbf{A}$ , respectively.  $\|\mathbf{A}\|_F$  and  $\text{tr}(\mathbf{A})$  represent the Frobenius norm and the trace of  $\mathbf{A}$ , respectively.  $\mathbf{I}_N$  represents an  $N \times N$  identity matrix.  $\mathcal{CN}(\mu, \sigma^2)$  denotes circularly symmetric complex Gaussian distribution with mean  $\mu$  and variance  $\sigma^2$ .  $U(a, b)$

The authors are with the CAS Key Laboratory of Wireless-Optical Communications, University of Science and Technology of China, Hefei 230027, China (e-mail: ruisun@mail.ustc.edu.cn; wdwang@ustc.edu.cn; chenli87@ustc.edu.cn; wei@ustc.edu.cn; wenyizha@ustc.edu.cn).

denotes uniform distribution over the interval  $[a, b]$ .

## II. SYSTEM MODEL

We consider an analog beamforming (ABF) mmWave massive MIMO system equipped with an  $N$ -element uniform linear array (ULA)<sup>1</sup>, which is the array-under-test (AUT). A single-antenna diagnostic transmitter (TX) is adopted to transmit test symbols. The AUT receives the test symbol and conducts the diagnosis. In the absence of antenna failure, the fault-free received symbol can be expressed as

$$y' = \mathbf{f}^T \mathbf{h} x + w, \quad (1)$$

where  $\mathbf{f} \in \mathbb{C}^N$  is the combining vector,  $\mathbf{h} \in \mathbb{C}^N$  is the channel vector between the TX and the AUT,  $x$  is the transmit symbol,  $w \sim \mathcal{CN}(0, 1/\text{SNR})$  is the noise and SNR is the signal-to-noise ratio.

The channel  $\mathbf{h}$  is assumed as the block-fading mmWave clustered channel [14], [15], which can be expressed as

$$\mathbf{h} = \sum_{l=1}^L \alpha_l \mathbf{a}(\theta_l), \quad (2)$$

where  $\mathbf{a}(\theta_l) = [1, e^{j2\pi d \sin \theta_l}, \dots, e^{j2\pi d(N-1) \sin \theta_l}]^T$  is the array response vector,  $L$  is the number of sub-paths,  $\alpha_l \sim \mathcal{CN}(0, 1/L)$  and  $\theta_l \sim U(-\pi/2, \pi/2)$  are the complex gain and the angle-of-arrival (AOA) of the  $l$ -th sub-path, respectively, and  $d = 1/2$  is the element spacing relative to the wavelength.

In the presence of faulty antenna elements, the actual channel vector will deviate from the ideal one. Therefore, the received symbol under antenna faults can be expressed as

$$y = \mathbf{f}^T (\mathbf{h} + \mathbf{h}_f) x + w, \quad (3)$$

where  $\mathbf{h}_f \in \mathbb{C}^N$  is the fault-induced channel deviation. Due to the *failure sparsity* that usually only a few antenna elements are faulty [4], [5],  $\mathbf{h}_f$  is assumed as a sparse vector, in which non-zero entries indicate faulty antenna elements.

To detect faults, the TX transmit test symbol  $x = 1$  throughout the diagnosis. Within the channel coherence time, the AUT uses  $K$  random combining vectors to receive the signal, yielding the observation model

$$\mathbf{y} = \mathbf{F}(\mathbf{h} + \mathbf{h}_f) + \mathbf{w}, \quad (4)$$

where

$$\begin{aligned} \mathbf{y} &= [y_1, \dots, y_K]^T \in \mathbb{C}^K, \\ \mathbf{F} &= [\mathbf{f}_1, \dots, \mathbf{f}_K]^T \in \mathbb{C}^{K \times N}, \\ \mathbf{w} &= [w_1, \dots, w_K]^T \in \mathbb{C}^K, \end{aligned} \quad (5)$$

in which  $y_k$ ,  $\mathbf{f}_k$ , and  $w_k$  are the received symbol, the combining vector, and the noise corresponded to the  $k$ -th measurement, respectively.

The goal of diagnosis is to recover the sparse fault-induced channel deviation  $\mathbf{h}_f$ , in which non-zero entries indicate faulty antenna elements. From (4), it can be observed that  $\mathbf{h}_f$  is coupled with the fault-free channel vector  $\mathbf{h}$ . Since the system

contains potentially faulty antenna elements, the channel vector  $\mathbf{h}$  can not be estimated by conventional channel estimation techniques like pilot-based training, and thus recovering  $\mathbf{h}_f$  under unknown  $\mathbf{h}$  can be challenging.

To cope with this issue, prior works require full or partial CSI knowledge to perform the diagnosis. The diagnostic technique proposed in [5] requires full CSI, which assumes a free-space wireless channel and proposes to calculate the channel vector using known sub-path AOA and gain (i.e.,  $\theta_l$  and  $\alpha_l$ ). Hence, one can generate the fault-free channel vector  $\mathbf{h}$  using (2) and subtract it from the received signal, and the impact of channel can be eliminated. A recent work [13] relaxes the CSI requirement in the sense that it only requires the AOA of each sub-path (i.e.,  $\theta_l$ ), whose main idea is to project the received signal onto the null space of AOAs and thus the impact of channel can also be eliminated.

It can be found that the above diagnostic techniques follow the routine of “cancel-then-recover” in the sense that they seek to cancel the impact of channel from the received signal first and then recover fault-induced channel deviation, which requires full or partial CSI knowledge. Such CSI assumption sometimes can be challenging to satisfy, especially for the outdoor online diagnosis in a complex multipath scattering environment. In the following, we propose a diagnostic technique that does not require any knowledge of the CSI (i.e., blind diagnosis). This is achieved by jointly exploiting the mmWave channel sparsity and the failure sparsity. Besides, the fault-free channel vector  $\mathbf{h}$  can also be recovered, which provides an approach to perform channel estimation under antenna element failures.

## III. FAULT DIAGNOSIS

### A. Problem Formulation

Recall that our goal is to recover  $\mathbf{h}$  and  $\mathbf{h}_f$  simultaneously under the observation model

$$\mathbf{y} = \mathbf{F}(\mathbf{h} + \mathbf{h}_f) + \mathbf{w}. \quad (6)$$

Intuitively speaking, it seems impossible to distinguish channel fading from antenna failures, and hence recovering  $\mathbf{h}$  and  $\mathbf{h}_f$  simultaneously can be a challenging task. To decouple the failure deviation  $\mathbf{h}_f$  from the channel  $\mathbf{h}$ , we need to exploit their structural characteristics. The fault-induced channel deviation  $\mathbf{h}_f$  is sparse itself due to the failure sparsity that only a few antenna elements are faulty. The ideal channel vector  $\mathbf{h}$  is also sparse in the Fourier dictionary since the mmWave channel is sparse in the angle domain (i.e.,  $L \ll N$ ) [14]. Therefore,  $\mathbf{h}$  and  $\mathbf{h}_f$  are sparse under different dictionaries, which allows them to be recovered simultaneously [16].

To jointly recover  $\mathbf{h}$  and  $\mathbf{h}_f$ , we need to introduce *a-priori* information on them. The fault-induced channel deviation  $\mathbf{h}_f$  is sparse itself. We adopt the well-known  $l_1$  norm as the sparsity-inducing norm for  $\mathbf{h}_f$ :

$$\|\mathbf{h}_f\|_1 = \sum_{n=1}^N |h_{f,n}|, \quad (7)$$

where  $h_{f,n}$  is the  $n$ -th entry in  $\mathbf{h}_f$ .

<sup>1</sup>The proposed diagnostic technique can be easily extended to other system architectures (like digital beamforming (DBF) and hybrid beamforming (HBF) systems) and other array structures (like uniform planar array (UPA)).

The ideal channel vector  $\mathbf{h}$  is sparse in the Fourier dictionary. To be more specific,  $\mathbf{h}$  is sparse in the continuous Fourier dictionary

$$\mathcal{A} = \{\mathbf{a}(\theta_l) | \theta_l \in [-\pi/2, \pi/2]\}. \quad (8)$$

We adopt the atomic norm as the sparsity-inducing norm for  $\mathbf{h}$ . The atomic norm of  $\mathbf{h}$  over the dictionary  $\mathcal{A}$  is defined as [17]

$$\|\mathbf{h}\|_{\mathcal{A}} = \inf \left\{ \sum_l |\alpha_l| \mid \mathbf{h} = \sum_l \alpha_l \mathbf{a}_l, \mathbf{a}_l \in \mathcal{A} \right\}, \quad (9)$$

which can be regarded as the  $l_1$  norm over the continuous dictionary  $\mathcal{A}$ .

Using the  $l_1$  norm and the atomic norm as sparsity-inducing norm for  $\mathbf{h}_f$  and  $\mathbf{h}$ , respectively, the optimization problem for joint recovery can be expressed as

$$\{\hat{\mathbf{h}}, \hat{\mathbf{h}}_f\} = \arg \min_{\mathbf{h}, \mathbf{h}_f} \frac{1}{2} \|\mathbf{y} - \mathbf{F}(\mathbf{h} + \mathbf{h}_f)\|_2^2 + \tau \|\mathbf{h}\|_{\mathcal{A}} + \lambda \|\mathbf{h}_f\|_1, \quad (10)$$

where  $\tau$  and  $\lambda$  are regularization parameters controlling the sparsity penalty on  $\mathbf{h}$  and  $\mathbf{h}_f$ , respectively. The optimization problem (10) tends to find a sparse vector  $\mathbf{h}_f$  and a vector  $\mathbf{h}$  that is sparse under the dictionary  $\mathcal{A}$  to fit the observation model.

Although the optimization problem (10) is clear in its form, it can not be directly solved since it involves infinite-dimensional variable optimization due to the continuity of the dictionary  $\mathcal{A}$ . To cope with this issue, a conventional approach is to discretize the angle domain into a grid, which forms a discrete Fourier transform (DFT) dictionary [18]. This approach, however, induces the off-grid error since the AOAs will not lie exactly on the grid, which may significantly degrades the recovery performance [19]. In the following, we develop an efficient algorithm for solving the optimization problem (10).

### B. An Efficient Diagnostic Algorithm

The main difficulty of solving (10) arises from the atomic norm  $\|\mathbf{h}\|_{\mathcal{A}}$  over the continuous Fourier dictionary  $\mathcal{A}$ . Fortunately, the minimization of  $\|\mathbf{h}\|_{\mathcal{A}}$  admits the following semidefinite program (SDP) thanks to the Carathéodory–Fejér–Pisarenko decomposition [17], [20]

$$\arg \min_{\substack{\mathbf{u} \in \mathbb{C}^N \\ v \in \mathbb{R}}} \frac{1}{2} \left( \frac{1}{N} \text{tr}(T(\mathbf{u})) + v \right) \quad \text{s.t.} \quad \begin{bmatrix} T(\mathbf{u}) & \mathbf{h} \\ \mathbf{h}^H & v \end{bmatrix} \succeq 0, \quad (11)$$

where  $\text{tr}(\cdot)$  denotes the trace of a matrix, and  $T(\mathbf{u})$  is the Hermitian Toeplitz matrix with vector  $\mathbf{u}$  as its first column.

Therefore, the optimization problem (10) has the equivalent SDP

$$\begin{aligned} \{\hat{\mathbf{h}}, \hat{\mathbf{h}}_f\} = \arg \min_{\mathbf{h}, \mathbf{h}_f, \mathbf{u}, v} & \frac{1}{2} \|\mathbf{y} - \mathbf{F}(\mathbf{h} + \mathbf{h}_f)\|_2^2 \\ & + \frac{\tau}{2} \left( \frac{1}{N} \text{tr}(T(\mathbf{u})) + v \right) + \lambda \|\mathbf{h}_f\|_1 \\ \text{s.t.} & \begin{bmatrix} T(\mathbf{u}) & \mathbf{h} \\ \mathbf{h}^H & v \end{bmatrix} \succeq 0. \end{aligned} \quad (12)$$

Related works on the atomic norm suggest using the CVX toolbox to solve the SDP (12) [17], which can be time-consuming for large-scale problems. To solve (12) in an efficient way, we develop an algorithm based on the alternating direction method of multipliers (ADMM) algorithm [21]. The ADMM algorithm integrates the augmented Lagrangian method with the dual ascent method, which shows excellent efficiency in solving large-scale problems.

We first rewrite (12) into the ADMM form:

$$\begin{aligned} \{\hat{\mathbf{h}}, \hat{\mathbf{h}}_f\} = \arg \min_{\mathbf{h}, \mathbf{h}_f, \mathbf{u}, v} & \frac{1}{2} \|\mathbf{y} - \mathbf{F}(\mathbf{h} + \mathbf{h}_f)\|_2^2 \\ & + \frac{\tau}{2} \left( \frac{1}{N} \text{tr}(T(\mathbf{u})) + v \right) + \lambda \|\mathbf{h}_f\|_1, \\ \text{s.t.} & \mathbf{Z} = \begin{bmatrix} T(\mathbf{u}) & \mathbf{h} \\ \mathbf{h}^H & v \end{bmatrix} \succeq 0, \end{aligned} \quad (13)$$

where  $\mathbf{Z} \in \mathbb{C}^{(N+1) \times (N+1)}$  is an auxiliary matrix.

The augmented Lagrangian function for (13) can be expressed as

$$\begin{aligned} \mathcal{L}_\rho(v, \mathbf{u}, \mathbf{h}, \mathbf{h}_f, \mathbf{Z}, \mathbf{\Lambda}) &= \frac{1}{2} \|\mathbf{y} - \mathbf{F}(\mathbf{h} + \mathbf{h}_f)\|_2^2 + \frac{\tau}{2} \left( \frac{1}{N} \text{tr}(T(\mathbf{u})) + v \right) + \lambda \|\mathbf{h}_f\|_1 \\ &+ \left\langle \mathbf{\Lambda}, \mathbf{Z} - \begin{bmatrix} T(\mathbf{u}) & \mathbf{h} \\ \mathbf{h}^H & v \end{bmatrix} \right\rangle + \frac{\rho}{2} \left\| \mathbf{Z} - \begin{bmatrix} T(\mathbf{u}) & \mathbf{h} \\ \mathbf{h}^H & v \end{bmatrix} \right\|_F^2, \end{aligned} \quad (14)$$

where  $\mathbf{\Lambda} \in \mathbb{C}^{(N+1) \times (N+1)}$  is the Lagrangian multiplier,  $\rho$  is a penalty parameter, and  $\langle \cdot, \cdot \rangle$  denotes the real inner product.

The ADMM algorithm minimizes the augmented Lagrangian function by iteratively updating the following variables:

$$\begin{aligned} v^{(l+1)} &= \arg \min_v \mathcal{L}_\rho(v, \mathbf{u}^{(l)}, \mathbf{h}^{(l)}, \mathbf{h}_f^{(l)}, \mathbf{Z}^{(l)}, \mathbf{\Lambda}^{(l)}), \\ \mathbf{u}^{(l+1)} &= \arg \min_{\mathbf{u}} \mathcal{L}_\rho(v^{(l+1)}, \mathbf{u}, \mathbf{h}^{(l)}, \mathbf{h}_f^{(l)}, \mathbf{Z}^{(l)}, \mathbf{\Lambda}^{(l)}), \\ \mathbf{h}^{(l+1)} &= \arg \min_{\mathbf{h}} \mathcal{L}_\rho(v^{(l+1)}, \mathbf{u}^{(l+1)}, \mathbf{h}, \mathbf{h}_f^{(l)}, \mathbf{Z}^{(l)}, \mathbf{\Lambda}^{(l)}), \\ \mathbf{h}_f^{(l+1)} &= \arg \min_{\mathbf{h}_f} \mathcal{L}_\rho(v^{(l+1)}, \mathbf{u}^{(l+1)}, \mathbf{h}^{(l+1)}, \mathbf{h}_f, \mathbf{Z}^{(l)}, \mathbf{\Lambda}^{(l)}), \\ \mathbf{Z}^{(l+1)} &= \arg \min_{\mathbf{Z}} \mathcal{L}_\rho(v^{(l+1)}, \mathbf{u}^{(l+1)}, \mathbf{h}^{(l+1)}, \mathbf{h}_f^{(l+1)}, \mathbf{Z}, \mathbf{\Lambda}^{(l)}), \\ \mathbf{\Lambda}^{(l+1)} &= \mathbf{\Lambda}^{(l)} + \rho \left( \mathbf{Z}^{(l+1)} - \begin{bmatrix} T(\mathbf{u}^{(l+1)}) & \mathbf{h}^{(l+1)} \\ \mathbf{h}^{(l+1)H} & v^{(l+1)} \end{bmatrix} \right), \end{aligned} \quad (15)$$

where the superscript  $(l)$  denotes the  $l$ -th iteration.

To perform the above updates in an explicit way, we first introduce the partitions

$$\mathbf{Z}^{(l)} = \begin{bmatrix} \mathbf{Z}_0^{(l)} & \mathbf{z}_1^{(l)} \\ \mathbf{z}_1^{(l)H} & Z_{N+1, N+1}^{(l)} \end{bmatrix}, \mathbf{\Lambda}^{(l)} = \begin{bmatrix} \mathbf{\Lambda}_0^{(l)} & \boldsymbol{\lambda}_1^{(l)} \\ \boldsymbol{\lambda}_1^{(l)H} & \Lambda_{N+1, N+1}^{(l)} \end{bmatrix}. \quad (16)$$

The augmented Lagrangian function is convex and differentiable with respect to the variables  $v$ ,  $\mathbf{u}$ , and  $\mathbf{h}$ . Setting their

gradient to zero, these updates have closed-form expressions

$$\begin{aligned} v^{(l+1)} &= Z_{N+1,N+1}^{(l)} + \frac{1}{\rho} \left( \Lambda_{N+1,N+1}^{(l)} - \frac{\tau}{2} \right), \\ \mathbf{u}^{(l+1)} &= \Psi^{-1} \left( T^* \left( \mathbf{Z}_0^{(l)} + \frac{1}{\rho} \Lambda_0^{(l)} \right) \right) - \frac{\tau}{2\rho} \mathbf{e}_1, \\ \mathbf{h}^{(l+1)} &= (\mathbf{F}^H \mathbf{F} + 2\rho \mathbf{I}_N)^{-1} \left( \mathbf{F}^H (\mathbf{y} - \mathbf{F} \mathbf{h}_f^{(l)}) + 2\lambda_1^{(l)} + 2\rho \mathbf{z}_1^{(l)} \right), \end{aligned} \quad (17)$$

where  $\Psi$  is a diagonal matrix and  $\Psi_{i,j} = N - j + 1, j = 1, \dots, N$ ,  $\mathbf{e}_1$  is a zero vector with the first entry being one, and  $T^*(\cdot)$  generates a vector whose  $i$ -th element is the trace of the  $(i-1)$ -th subdiagonal of the input matrix.

The update of  $\mathbf{h}_f$  can be written as

$$\mathbf{h}_f^{(l+1)} = \arg \min_{\mathbf{h}_f} \frac{1}{2} \|\mathbf{y} - \mathbf{F} \mathbf{h}^{(l+1)} - \mathbf{F} \mathbf{h}_f\|_2^2 + \lambda \|\mathbf{h}_f\|_1, \quad (18)$$

which is the well-known LASSO problem and can be solved efficiently by the algorithm proposed in [21].

Finally, the update of  $\mathbf{Z}$  can be expressed as

$$\mathbf{Z}^{(l+1)} = \arg \min_{\mathbf{Z} \succeq 0} \left\| \mathbf{Z} - \underbrace{\begin{pmatrix} T(\mathbf{u}^{(l+1)}) & \mathbf{h}^{(l+1)} \\ \mathbf{h}^{(l+1)H} & v^{(l+1)} \end{pmatrix} - \frac{1}{\rho} \Lambda^{(l)}}_{\mathbf{G}} \right\|_{\mathbf{F}}^2, \quad (19)$$

which amounts to projecting the Hermitian matrix  $\mathbf{G}$  onto the positive semidefinite cone and can be performed by computing the eigenvalue decomposition of  $\mathbf{G}$  and setting all negative eigenvalues to zero.

The overall algorithm for solving (12) is summarized in Algorithm 1. The computational complexity mainly arises from the updates of  $\mathbf{h}$ ,  $\mathbf{h}_f$ , and  $\mathbf{Z}$ . The updates of  $\mathbf{h}$  and  $\mathbf{h}_f$  involve matrix inversion, which has the complexity of  $O(N^3)$ . The update of  $\mathbf{Z}$  requires eigenvalue decomposition and has the complexity of  $O((N+1)^3)$ . Therefore, the update of  $\mathbf{Z}$  dominates the overall computational complexity and we have  $O((N+1)^3)$  for Algorithm 1.

#### IV. NUMERICAL SIMULATIONS

In this section, we conduct numerical simulations to evaluate the performance of proposed diagnostic technique. The number of antenna elements is set to  $N = 64$ . The number of faulty antenna elements is set to 3, whose locations are chosen uniformly at random. The amplitude and phase of the entries in the fault-induced channel deviation  $\mathbf{h}_f$  follow  $U(0.2, 1)$  and  $U(0, 2\pi)$ , respectively. We adopt the success probability as the performance metric, which is defined as the probability that the status of all antenna elements is correctly identified. For comparison, we adopt the diagnostic techniques proposed in [5] (denoted as Eltayeb18) and [13] (denoted as Medina20) as benchmark techniques, which require full and partial CSI, respectively.

First, we evaluate the effect of the number of measurements. Fig. 1 shows the success probability versus the number of measurements under different SNRs, where the number of sub-paths is set to  $L = 4$ . It can be observed that all techniques perform better with a larger number of measurements and/or

#### Algorithm 1: An Efficient Algorithm for Solving (12)

---

Initialization:  $\mathbf{Z}^{(0)} = \mathbf{0}$ ,  $\Lambda^{(0)} = \mathbf{0}$ ,  $\mathbf{h}_f^{(0)} = \mathbf{0}$ ;  
**while not converged do**  
1  $v^{(l+1)} = Z_{N+1,N+1}^{(l)} + \frac{1}{\rho} \left( \Lambda_{N+1,N+1}^{(l)} - \frac{\tau}{2} \right)$ ;  
2  $\mathbf{u}^{(l+1)} = \Psi^{-1} \left( T^* \left( \mathbf{Z}_0^{(l)} + \frac{1}{\rho} \Lambda_0^{(l)} \right) \right) - \frac{\tau}{2\rho} \mathbf{e}_1$ ;  
3  $\mathbf{h}^{(l+1)} = (\mathbf{F}^H \mathbf{F} + 2\rho \mathbf{I}_N)^{-1} \left( \mathbf{F}^H (\mathbf{y} - \mathbf{F} \mathbf{h}_f^{(l)}) + 2\lambda_1^{(l)} + 2\rho \mathbf{z}_1^{(l)} \right)$ ;  
4  $\mathbf{h}_f^{(l+1)} = \arg \min_{\mathbf{h}_f} \frac{1}{2} \|\mathbf{y} - \mathbf{F} \mathbf{h}^{(l+1)} - \mathbf{F} \mathbf{h}_f\|_2^2 + \lambda \|\mathbf{h}_f\|_1$ , which is the LASSO problem and can be solved by the algorithm proposed in [21];  
5 Perform eigenvalue decomposition on  $\begin{bmatrix} T(\mathbf{u}^{(l+1)}) & \mathbf{h}^{(l+1)} \\ \mathbf{h}^{(l+1)H} & v^{(l+1)} \end{bmatrix} - \frac{1}{\rho} \Lambda^{(l)}$  and set all negative eigenvalues to zero, yielding  $\mathbf{Z}^{(l+1)}$ ;  
6  $\Lambda^{(l+1)} = \Lambda^{(l)} + \rho \left( \mathbf{Z}^{(l+1)} - \begin{bmatrix} T(\mathbf{u}^{(l+1)}) & \mathbf{h}^{(l+1)} \\ \mathbf{h}^{(l+1)H} & v^{(l+1)} \end{bmatrix} \right)$ ;  
**end**

---

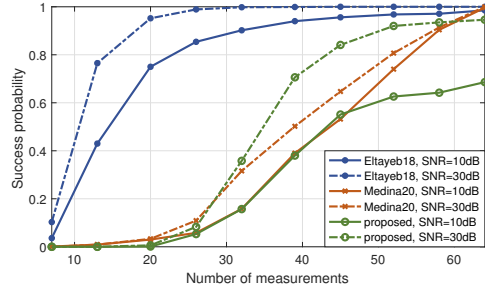


Fig. 1. Success probability versus the number of measurements under different SNRs.

larger SNR. Among all diagnostic techniques, the diagnosis with full CSI (Eltayeb18) outperforms others since the impact of channel can be completely eliminated using known CSI. When the SNR is sufficiently large, the proposed technique has slightly better performance than the diagnosis with partial CSI (Medina20).

Next, we assume that the estimated sub-path gain  $\hat{\alpha}_l$  contains estimation error, which is defined as

$$\hat{\alpha}_l = \alpha_l + \delta_\alpha \alpha_e, \quad (20)$$

where  $\alpha_e \sim \mathcal{CN}(0, 1)$  represents gain estimation error and  $\delta_\alpha$  is the error intensity. The performance of different techniques under sub-path gain estimation error is shown in Fig. 2, where  $\text{SNR} = 30\text{dB}$  and the number of measurements is set to  $K = N$  to ensure sufficient measurements for all techniques. We can observe that the performance of diagnosis with full CSI (Eltayeb18) degrades significantly under gain estimation errors, while other techniques are not affected by the estimation error since they do not require the knowledge of sub-path gain. Besides, the more sub-paths in the channel, the

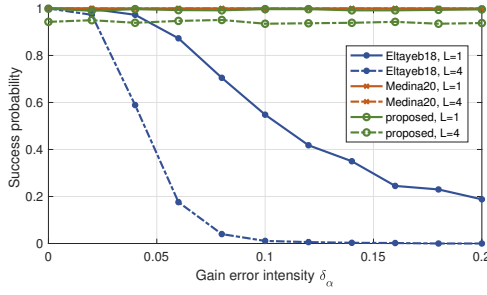


Fig. 2. Success probability versus sub-path gain error intensity under different number of sub-paths.

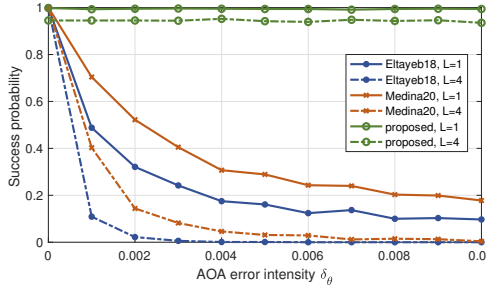


Fig. 3. Success probability versus sub-path AOA error intensity under different number of sub-paths.

worse the performance since more errors will be introduced.

Finally, we assume that the estimated AOA  $\hat{\theta}_l$  contains estimation error, which is defined as

$$\hat{\theta}_l = \theta_l + \delta_\theta \theta_e \pi, \quad (21)$$

where  $\theta_e \sim \mathcal{N}(0, 1)$  represents the AOA estimation error and  $\delta_\theta$  is the error intensity. The success probabilities of different techniques under AOA estimation error are shown in Fig. 3, where SNR = 30dB and the number of measurements is set to  $K = N$ . It can be observed that benchmark diagnostic techniques are highly sensitive to AOA estimation errors. On the contrary, the performance of proposed diagnostic technique is not affected under all intensities of AOA estimation error since it does not require any CSI knowledge, which shows strong robustness against channel estimation errors.

## V. CONCLUSIONS

In this letter, we have proposed a blind diagnostic technique for mmWave massive MIMO systems to locate faulty antenna elements. By jointly exploiting the sparsity of the mmWave channel and the failure, the location of faulty antenna elements can be identified without any knowledge of the CSI. A novel atomic norm has been introduced as the sparsity-inducing norm of the mmWave channel, and the diagnosis problem has been formulated as a joint sparse recovery problem. An efficient ADMM-based diagnostic algorithm has been proposed to solve the joint sparse recovery problem. Numerical results have shown that the proposed technique has strong robustness against channel estimation errors compared with prior works, which provides a practical approach for the outdoor online diagnosis.

## REFERENCES

- [1] G. G. Fischer and S. Glisic, "Temperature stability and reliability aspects of 77 GHz voltage controlled oscillators in a SiGe: C BiCMOS technology," in *IEEE Topical Meeting on Silicon Monolithic Integrated Circuits in RF Systems*. IEEE, 2008, pp. 171–174.
- [2] W. Chang, J. Luo, Y. Qi, and B. Wang, "Reliability and failure analysis in designing a typical operation amplifier," in *17th IEEE International Symposium on the Physical and Failure Analysis of Integrated Circuits*. IEEE, 2010, pp. 1–4.
- [3] E. Vinyaikin, M. Zinicheva, and A. Naumov, "Attenuation and phase variation of millimeter and centimeter radio waves in a medium consisting of dry and wet dust particles," *Radiophys. Quantum Electron.*, vol. 37, no. 11, pp. 914–923, 1994.
- [4] M. D. Migliore, "A compressed sensing approach for array diagnosis from a small set of near-field measurements," *IEEE Trans. Antennas Propag.*, vol. 59, no. 6, pp. 2127–2133, 2011.
- [5] M. E. Eltayeb, T. Y. Al-Naffouri, and R. W. Heath, "Compressive sensing for millimeter wave antenna array diagnosis," *IEEE Trans. Commun.*, vol. 66, no. 6, pp. 2708–2721, 2018.
- [6] R. Palmeri, T. Isernia, and A. F. Morabito, "Diagnosis of planar arrays through phaseless measurements and sparsity promotion," *IEEE Antennas Wirel. Propag. Lett.*, vol. 18, no. 6, pp. 1273–1277, 2019.
- [7] C. Xiong, G. Xiao, Y. Hou, and M. Hameed, "A compressed sensing-based element failure diagnosis method for phased array antenna during beam steering," *IEEE Antennas Wirel. Propag. Lett.*, vol. 18, no. 9, pp. 1756–1760, 2019.
- [8] T. Ince and G. Ögücü, "Array failure diagnosis using nonconvex compressed sensing," *IEEE Antennas Wirel. Propag. Lett.*, vol. 15, pp. 992–995, 2015.
- [9] M. Salucci, A. Gelmini, G. Oliveri, and A. Massa, "Planar array diagnosis by means of an advanced Bayesian compressive processing," *IEEE Trans. Antennas Propag.*, vol. 66, no. 11, pp. 5892–5906, 2018.
- [10] S. Ma, W. Shen, J. An, and L. Hanzo, "Antenna array diagnosis for millimeter-wave MIMO systems," *IEEE Trans. Veh. Technol.*, vol. 69, no. 4, pp. 4585–4589, 2020.
- [11] K. Chen, W. Wang, X. Chen, and H. Yin, "Deep learning based antenna array fault detection," in *IEEE 89th Vehicular Technology Conference (VTC2019-Spring)*. IEEE, 2019, pp. 1–5.
- [12] R. Sun, W. Wang, L. Chen, G. Wei, and W. Zhang, "Hybrid beamforming system diagnosis: Failure modeling and identification," *IEEE Trans. Wireless Commun.*, 2020.
- [13] G. Medina, A. S. Jida, S. Pulipati, R. Talwar, T. Y. Al-Naffouri, A. Madanayake, M. Eltayeb *et al.*, "Millimeter-wave antenna array diagnosis with partial channel state information," *arXiv preprint arXiv:2011.00828*, 2020.
- [14] M. R. Akdeniz, Y. Liu, M. K. Samimi, S. Sun, S. Rangan, T. S. Rappaport, and E. Erkip, "Millimeter wave channel modeling and cellular capacity evaluation," *IEEE J. Sel. Areas Commun.*, vol. 32, no. 6, pp. 1164–1179, 2014.
- [15] A. Alkhateeb, O. El Ayach, G. Leus, and R. W. Heath, "Channel estimation and hybrid precoding for millimeter wave cellular systems," *IEEE J. Sel. Top. Signal Process.*, vol. 8, no. 5, pp. 831–846, 2014.
- [16] M. F. Duarte, M. A. Davenport, M. B. Wakin, and R. G. Baraniuk, "Sparse signal detection from incoherent projections," in *IEEE International Conference on Acoustics Speech and Signal Processing Proceedings*, vol. 3. IEEE, 2006, pp. III–III.
- [17] G. Tang, B. N. Bhaskar, P. Shah, and B. Recht, "Compressed sensing off the grid," *IEEE Trans. Inf. Theory*, vol. 59, no. 11, pp. 7465–7490, 2013.
- [18] Z. Yang, L. Xie, and C. Zhang, "Off-grid direction of arrival estimation using sparse Bayesian inference," *IEEE Trans. Signal Process.*, vol. 61, no. 1, pp. 38–43, 2012.
- [19] Y. Chi, L. L. Scharf, A. Pezeshki, and A. R. Calderbank, "Sensitivity to basis mismatch in compressed sensing," *IEEE Trans. Signal Process.*, vol. 59, no. 5, pp. 2182–2195, 2011.
- [20] T. T. Georgiou, "The carathéodory–fejér–pisarenko decomposition and its multivariable counterpart," *IEEE Trans. Autom. Control*, vol. 52, no. 2, pp. 212–228, 2007.
- [21] S. Boyd, N. Parikh, and E. Chu, *Distributed optimization and statistical learning via the alternating direction method of multipliers*. Now Publishers Inc, 2011.